Asociación Argentina
de Mecánica Computacional

Mecánica Computacional Vol XXXI, págs. 651-671 (artículo completo)
Alberto Cardona, Paul H. Kohan, Ricardo D. Quinteros, Mario A. Storti (Eds.)
Salta, Argentina, 13-16 Noviembre 2012

SOLVING THE ALGEBRAIC SLIP MIXTURE MODEL AS A HYPERBOLIC SYSTEM WITH RESTRICTIONS

Santiago Márquez Damián[a], **Norberto M. Nigro**[a] **and Gustavo C. Buscaglia**[b]

[a]*International Center for Computational Methods in Engineering (CIMEC), INTEC-UNL/CONICET, Güemes 3450, Santa Fe, Argentina, santiagomarquezd@gmail.com, http://www.cimec.org.ar*

[b]*Instituto de Ciências Matemáticas e de Computação (ICMC), Av. do Trabalhador Sãocarlense 400, Centro, CEP 13560-970 São Carlos, SP, Brasil,http://www.icmc.usp.br/*

Keywords: Multiphase Flow, Algebraic Slip Mixture Model, Hyperbolic Systems

Abstract. In this work the well established Algebraic Slip Mixture Model (ASMM) is revisited and studied. Since its presentation the related literature is centered in its derivation and the analysis of the closure laws needed for practical applications. In addition a rich mathematical and modelistic structure is present is this model. This structure is not much discussed, but is also valuable for the model implementation and use, particularly for high disperse-phase fractions.

So that, the incompressible ASMM is presented as a hyperbolic system with restrictions derived from the Two-Fluid model. The structure of the hyperbolic system is described, particularly the restriction given by the mixture mass conservation equation as is usual in incompressible problems, the importance of the dispersed phase conservation equation with the corresponding eigenvalue analysis and the cases obtained for two different dispersed-phase flux functions. A numerical solver is implemented based on this analysis taking into account the eigenvalues information for the correct stabilization and the issues related with the incompressibility, which is treated by pressure correction methods.

The analysis allows to derive a semi-analytical solution for sedimentation cases and the consequent validation of the numerical solver designed for the problem.

1 INTRODUCTION

In the solution of interpenetrated multiphase flows, two models are widely used, the Multi-Fluid model and its simplification given by the Algebraic Slip Mixture Model (ASMM) (Ishii and Hibiki, 2010). Even when ASMM is physically more limited its results are sometimes comparable to the Multi-Fluid model due the lack of closure laws available for the last one. This feature and its simplicity make this method suitable for accurate and fast solution in cyclones and plume problems (Qian et al., 2007; Buscaglia et al., 2002).

The foundation and most cited works about ASMM (Ishii, 1975; Manninen et al., 1996) are centered in its derivation and the hypothesis and laws for the interactions between the different phases. The secondary phases are often considered as particulated phases, such that droplets, bubbles or solid particles, so that these laws are related with drag phenomena.

In addition to the comprehension of the physical basis of the equations and the necessity of closure laws, the implementation of ASMM requires to circumvent some numerical and algorithmic issues. The first one consists in the limitation given by the lack of existence of an equation for the pressure. In other mixture models it is often solved by an Equation of State, which gives an algebraic relationship between the pressure and the density (Zeidan and Slaouti, 2009; Zeidan, 2011). In the case of ASMM the problem is normally assumed as incompressible, so that, the pressure is a Lagrange Multiplier for the restriction given by the mass conservation equation of the mixture (Gastaldo et al., 2008). This issue appears also in reacting flows (Babik et al., 2005; Najm et al., 1998; Knio et al., 1999), the Low-Mach solvers applied to this problem are also an inspiration for the solution of ASMM problems. The other important aspect is the necessity of a proper integration of the secondary phases transport equations, in order to ensure the boundedness and the conservation of the mass of each phase (Gastaldo et al., 2011).

With the aim of sum up to the discussion this work recalls the nature of ASMM as a hyperbolic system with restrictions and discusses the methods used for the solution proposing a new solver based on the PISO method (Issa, 1986). In addition, an original semi-analytical solution for a sedimentation case is presented, which serves as a validation for the solver.

2 THE ALGEBRAIC SLIP MIXTURE MODEL

The Algebraic Slip Mixture Model is a multi-phase model for n interpenetrated phases based on the multi-fluid model (Ishii, 1975; Ishii and Hibiki, 2010). In this model all the phases are treated as a mixture which exhibits mean properties for density and viscosity. In the multi-fluid model a mass and momentum equation are solved for each phase, on the other hand the ASMM reduces the system to a mass and momentum equation for the whole mixture and one mass conservation equation for $n-1$ phases. In addition, *algebraic* relations from each phase velocities respect to the mixture velocity are given and a closure law for all phases volume fractions is finally included. The complete derivation of the model is treated in full extension in the work of Manninen *et al.* (Manninen et al., 1996). Then, recalling this work, and using the so-called center-of-mass velocity formulation, the ASMM model can be written as follows.

The continuity equation for the mixture is given by Eqn. (1)

$$\frac{\partial}{\partial t}(\rho_m) + \vec{\nabla} \cdot (\rho_m \vec{v}_m) = 0 \tag{1}$$

where $\vec{v}_m$ is the velocity of center of mass defined by Eqn. (2)

$$\vec{v}_m = \frac{\sum_{k=1}^{n} \alpha_k \rho_k \vec{v}_k}{\rho_m} \tag{2}$$

and ρ_m the mixture density defined by Eqn. (3)

$$\rho_m = \sum_{k=1}^{n} \alpha_k \rho_k \tag{3}$$

where α_k is the volume fraction of phase k and n the number of phases. The mixture momentum is obtained by the summation of each phase momentum equation as it is explained in (Manninen et al., 1996). See Eqn. 4.

$$\frac{\partial}{\partial t}(\rho_m \vec{v}_m) + \vec{\nabla} \cdot (\rho_m \vec{v}_m \otimes \vec{v}_m) = -\vec{\nabla} p + \vec{\nabla} \cdot \left[\mu_m \left(\vec{\nabla} \vec{v}_m + \vec{\nabla} \vec{v}_m^{\mathrm{T}} \right) \right] + \rho_m \vec{g} + \vec{F} - \vec{\nabla} \cdot \left(\sum_{k=1}^{n} \alpha_k \rho_k \vec{v}_{\mathrm{dr},k} \otimes \vec{v}_{\mathrm{dr},k} \right) \tag{4}$$

where $\vec{F}$ is a body force, and μ_m is the dynamic viscosity of the mixture given by Eqn. (5)

$$\mu_m = \sum_{k=1}^{n} \alpha_k \mu_k \tag{5}$$

and $\vec{v}_{\mathrm{dr},k}$ is the drift velocity (relative velocity between k phase velocity and the velocity of center of mass, see Figure 1) for the secondary phase k which is defined by Eqn. 6.

$$\vec{v}_{\mathrm{dr},k} = \vec{v}_k - \vec{v}_m \tag{6}$$

The Drift velocity has no physical meaning but can be related to the relative velocity (See Figure 1) for a secondary phase (p) respect to the primary phase (q). So, the relative velocity, $\vec{v}_{pq}$ is defined by Eqn. 7

$$\vec{v}_{pq} = \vec{v}_p - \vec{v}_q \tag{7}$$

Now, defining the mass fraction for any phase (k) as in Eqn. (8)

$$c_k = \frac{\alpha_k \rho_k}{\rho_m} \tag{8}$$

is possible to relate the drift velocity and the relative velocity ($\vec{v}_{pq}$) by Eqn. (9):

$$\vec{v}_{\mathrm{dr},p} = \vec{v}_{pq} - \sum_{k=1}^{n} c_k \vec{v}_{qk} \tag{9}$$

In the case of having only one disperse phase Eqn. (9) can be written in a simpler form [See (Manninen et al., 1996) Eqn. (27)] as in Eqn. (10)

$$\vec{v}_{\mathrm{dr},p} = \vec{v}_{pq} \ (1 - c_p) \tag{10}$$

where c_p is the mass fraction for the disperse phase.

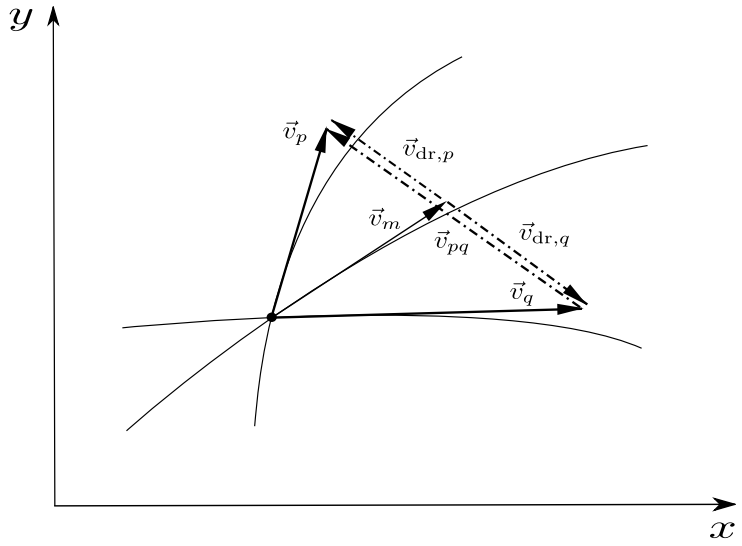

Figure 1: Example for the relation between the velocity of center of mass $\vec{v}_m$, relative $\vec{v}_{pq}$ and drift velocities $\vec{v}_{\mathrm{dr},p}$ and $\vec{v}_{\mathrm{dr},q}$ [adapted from (Ishii and Hibiki, 2010)]

Using the assumption that local equilibrium is reached in a short spatial length scale it is possible to use an algebraic formulation for relative velocities. This formulation depends on the physics of the problem, one of the most used one is that was given by Schiller & Naumann (Schiller and Naumann, 1935) which is centered in the drag law for particulate dispersed phases. In this work a more general expression will be used suitable for analytical manipulations.

Finally, it is necessary to have an equation for the evolution of the secondary phases. Starting from the continuity equation for secondary phase p, the volume fraction equation for this phase can be obtained (Eqn. 11):

$$\frac{\partial}{\partial t}(\alpha_p \rho_p) + \vec{\nabla} \cdot (\alpha_p \rho_p \vec{v}_m) = -\vec{\nabla} \cdot (\alpha_p \rho_p \vec{v}_{\mathrm{dr},p}) \tag{11}$$

The obtained system of equations for mixture mass, momentum and secondary phase mass conservation can be written for a two component mixture (gas-liquid) [see (Manninen et al., 1996), section 3.5.1], so that:

$$\begin{cases} \frac{\partial}{\partial t}(\rho_m) + \vec{\nabla} \cdot (\rho_m \vec{v}_m) = 0 \\ \\ \frac{\partial}{\partial t}(\rho_m \vec{v}_m) + \vec{\nabla} \cdot (\rho_m \vec{v}_m \otimes \vec{v}_m) = -\vec{\nabla} p + \vec{\nabla} \cdot \left[\mu_m \left(\vec{\nabla} \vec{v}_m + \vec{\nabla} \vec{v}_m^{\mathrm{T}} \right) \right] + \\ \qquad\qquad\qquad\qquad \rho_m \vec{g} - \vec{\nabla} \cdot \left[\rho_m c_p \left(1 - c_p \right) \vec{v}_{pq} \otimes \vec{v}_{pq} \right] \\ \\ \frac{\partial}{\partial t}(\alpha_g) + \vec{\nabla} \cdot (\alpha_g \vec{v}_m) = -\vec{\nabla} \cdot \left[\alpha_g \left(1 - c_p \right) \vec{v}_{pq} \right] \end{cases} \tag{12}$$

where the subindex g indicates the gas phase, $c_p = \alpha_g \, \rho_g / \rho_m$ the gas phase mass fraction.

This system of three equations has three unknowns, they are: $\vec{v}_m$, p and α_g. Respect to ρ_m it is linked to α_g via its constitutive equation, Eqn. (3). As is usual in incompressible problems the pressure has no evolution equation, so that it becomes a Lagrange Multiplier for the restriction

given by the mixture density transport equation. This characteristic leads to Fractional-Step or PISO/SIMPLE like methods (Babik et al., 2005; Gastaldo et al., 2008). In addition α_g has to be bounded in the [0, 1] interval to have physical meaning. Due to the fact of v_m is not divergence free the boundedness of α_g is not a direct consequence of the third equation in Eqn. (12), but of the whole system (Gastaldo et al., 2011).

The equation system obtained for gas-liquid mixture [Eqn. (12)] can be written in 1D. In addition, if the inviscid case is taken into account the results are then expressed like in the system [Eqn.(13)].

$$\begin{cases} \frac{\partial}{\partial t}(\rho_m) + \frac{\partial}{\partial z}(\rho_m v_m) = 0 \\ \\ \frac{\partial}{\partial t}(\rho_m v_m) + \frac{\partial}{\partial z}(\rho_m v_m v_m) = -\frac{\partial}{\partial z}p - \frac{\partial}{\partial z}\left[\rho_m c_p \left(1 - c_p\right) v_{pq}^2\right] + \rho_m \vec{g} \\ \\ \frac{\partial}{\partial t}(\alpha_g) + \frac{\partial}{\partial z}\left\{\alpha_g \left[v_m + \left(1 - c_p\right) v_{pq}\right]\right\} = 0 \end{cases} \tag{13}$$

The hypothesis of inviscid flux is based on the fact that all viscous effects related to the dispersed phase are taken into account in the relative velocity definition. In addition the effects of the mixture viscosity are zero in the transversal direction since no profile is developed in a one dimensional problem. The remaining term in the axial direction has marginal importance such as was proved using a viscous solver in the same experimental conditions.

2.1 The role of α_g equation

As it was stated previously the α_g equation represents the mass conservation of the secondary, dispersed phase. Its relevance is particularly important when the dynamics of the problem depend strongly in the evolution of the phases. As the first step in the analysis let's set the constitutive law for the relative velocity v_{pq} as it is shown in Eqn. (14)

$$v_{pq} = v_{rc}\ \left(1 - \alpha_g\right)^a \tag{14}$$

where v_{rc} and a are constants for the model. This expression is flexible and allows to match several other models, for example the Schiller & Naumann drag law can be fitted selecting an appropriate value for v_{rc} and with $0 \leqslant a \leqslant 1$ (Márquez Damián, 2012). Other constitutive law of this kind is that given by Barcelo *et al.* (L.F.Barceló et al., 2010) for their study of water-petroleum segregation.

The α_g equation can be finally written as in Eqn. (15)

$$\frac{\partial}{\partial t}(\alpha_g) + \frac{\partial}{\partial z}\mathrm{F}\left(\alpha_g\right) = \frac{\partial}{\partial t}(\alpha_g) + \frac{\partial}{\partial z}\left\{\alpha_g \left[v_m + \left(1 - \frac{\alpha_g\, \rho_g}{\rho_m}\right) v_{rc}\ \left(1 - \alpha_g\right)^a\right]\right\} = 0 \tag{15}$$

where $\mathrm{F}\left(\alpha_g\right)$ is the flux for this hyperbolic equation. It is, in general, a non-convex flux, so that, single and compound waves can be present as a part of the solution (LeVeque, 2002). The kind of waves depends on the relative velocity selected law (v_{pq}) and the particular initial conditions for each problem. This information is crucial to apply the necessary stabilization for advective terms.

3 ONE DIMENSIONAL SEMI-ANALYTICAL SOLUTION FOR SEDIMENTATION

Starting from the formulation of ASMM in 1D and under particular boundary conditions it is possible to arrive to a semi-analytical solution for the system given in Eqn. (13). The considered case consists in the sedimentation of a mixture of two fluids with different density, starting from a domain completely filled with the mixture, which is shown in Figure 2.

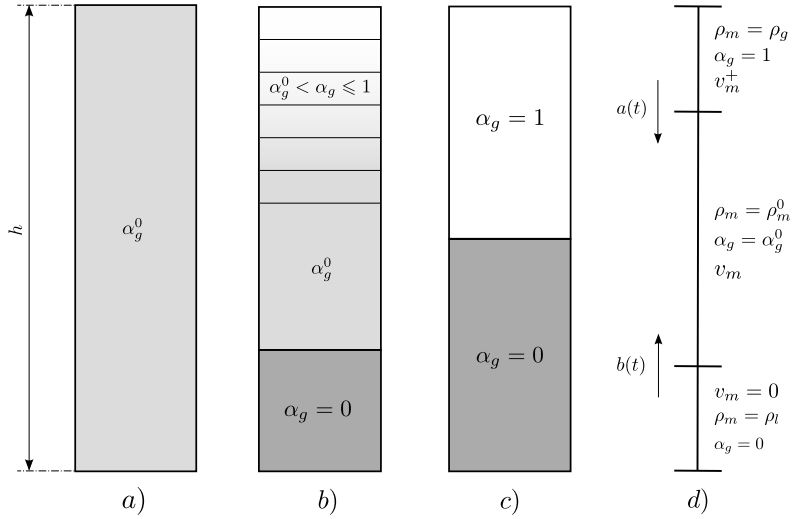

Figure 2: Simple sedimentation experiment. *a)* Initial conditions; *b)* settling transitory; *c)* steady state and *d)* simple scheme of problem variables

The mixture is composed by two fluids, the more dense phase with density ρ_l and the dispersed, less dense phase, with density ρ_g. α_g represents the volume fraction of the dispersed phase. Starting from the initial condition with $\alpha_g = \alpha_g^0$ and due to buoyancy the less dense phase goes up and the more dense phase settles at the bottom of the domain. The dynamics of the problem is governed by the relative velocity law, $v_{pq}(\alpha_g)$.

3.1 Determination of center-of-mass velocity

From the mixture density conservation equation in Eqn. (13) (first equation) and the constitutive equation for the mixture density in Eqn. (3) we have Eqn. (16)

$$\frac{\partial}{\partial t}(\rho_m) + \frac{\partial}{\partial z}(\rho_m v_m) = 0 \qquad \rho_m = \alpha_p \rho_g + (1 - \alpha_g)\,\rho_l \tag{16}$$

Now, taking the temporal derivative of ρ_m we obtain

$$\frac{\partial}{\partial t}(\rho_m) = (\rho_g - \rho_l)\frac{\partial}{\partial t}(\alpha_g) \tag{17}$$

this expression requires the evaluation of the temporal derivative of α_g which can be extracted from the α_g conservation equation in Eqn. (13) (third equation)

$$\frac{\partial}{\partial t}(\alpha_g) + \frac{\partial}{\partial z}\left\{\alpha_g\left[v_m + (1 - c_p)\,v_{pq}\right]\right\} = \frac{\partial}{\partial t}(\alpha_g) + \frac{\partial}{\partial z}\left(\alpha_g\, v_p\right) = 0 \tag{18}$$

isolating the temporal derivative

$$\frac{\partial}{\partial t}(\alpha_g) = -\frac{\partial}{\partial z}\left(\alpha_g\, v_p\right) \tag{19}$$

so that replacing this value in Eqn. (17) we have a new expression for the temporal derivative of mixture density

$$\frac{\partial}{\partial t}(\rho_m) = (\rho_l - \rho_g)\frac{\partial}{\partial z}(\alpha_g\, v_p) \tag{20}$$

which can be used in the conservation equation for the mixture density, Eqn. (16)

$$\frac{\partial}{\partial t}(\rho_m) + \frac{\partial}{\partial z}(\rho_m v_m) = (\rho_l - \rho_g)\frac{\partial}{\partial z}(\alpha_g\, v_p) + \frac{\partial}{\partial z}(\rho_m v_m) = 0 \tag{21}$$

or

$$\frac{\partial}{\partial z}\left[(\rho_l - \rho_g)\,(\alpha_g\, v_p) + (\rho_m v_m)\right] = 0 \tag{22}$$

in addition, being $v_p = v_m + (1 - c_p)\, v_{pq}$ then the last expression becomes

$$\frac{\partial}{\partial z}\left\{\left[(\rho_l - \rho_g)\,(\alpha_g\, v_p) + (\rho_m v_m)\right] + \left[\alpha_g\rho_g + (1-\alpha_g)\rho_l\right] v_m\right\} = 0 \tag{23}$$

This expression indicates that the argument of the derivative is constant in space. If we assume that for $z = 0$, $v_m = 0$ and $\alpha_g = 0$ (no slip wall and perfect settling at the bottom) this constant is zero, then, we have:

$$\left[(\rho_l - \rho_g)\,(\alpha_g\, v_p) + (\rho_m v_m)\right] + \left[\alpha_g\rho_g + (1-\alpha_g)\rho_l\right] v_m = 0 \tag{24}$$

next, with some extra algebra, the final expression results to be given by Eqn. (25)

$$v_m = \alpha_g\left(\frac{\rho_g}{\rho_m} - 1\right) v_{pq} \tag{25}$$

Now the value of v_m is linked algebraically to α_g so that, the solution of α_g implies the solution of v_m. To this end, it is necessary to select a law for v_{pq}.

3.2 Determination of the secondary phase void fraction

Recalling the third equation in Eqn. (13) it reads [Eqn. (26)]:

$$\frac{\partial}{\partial t}(\alpha_g) + \frac{\partial}{\partial z}\left\{\alpha_g\left[v_m + (1 - c_p)\, v_{pq}\right]\right\} = 0 \tag{26}$$

expanding the terms using their constitutive equations it results in Eqn. (27)

$$\frac{\partial}{\partial t}(\alpha_g) + \frac{\partial}{\partial z}\left\{\alpha_g\left[v_m + \left(1 - \frac{\alpha_g\,\rho_g}{\rho_m}\right) v_{rc}\,(1-\alpha_g)^a\right]\right\} = 0 \tag{27}$$

Here, using the expression obtained for v_m [Eqn. (25)] it is possible to arrive to the final equation for α_g [Eqn. (28)]

$$\frac{\partial}{\partial t}(\alpha_g) + \frac{\partial}{\partial z}\left\{\alpha_g\left[\alpha_g\left(\frac{\rho_g}{\rho_m} - 1\right) + \left(1 - \frac{\alpha_g\,\rho_g}{\rho_m}\right)\right] v_{rc}\,(1-\alpha_g)^a\right\} = 0 \tag{28}$$

once again it requires the selection of a law for v_{pq} based on the physics of the problem. The final expression of the α_g equation is a non-linear hyperbolic equation. The solution of this equation strongly depends on the definition of the flux, in this case, it reads [Eqn. (29)]

$$\mathrm{F}\left(\alpha_g\right) = \alpha_g \left[\alpha_g \left(\frac{\rho_g}{\rho_m} - 1\right) + \left(1 - \frac{\alpha_g\, \rho_g}{\rho_m}\right)\right] v_{rc}\, \left(1-\alpha_g\right)^a = v_{rc}\, \left(\alpha_g - \alpha_g^2\right)\, \left(1-\alpha_g\right)^a \tag{29}$$

The existence of different kind of waves in the solution leads to deal with one or more *Riemann problems* and requires appropriate methods for solving them (LeVeque, 2002; Toro, 2009). As is shown the flux doesn't depends explicitly on the physical parameters. The physics is included in the definitions of v_{rc} and the exponent a.

3.3 Determination of the pressure

Finally, the pressure of the problem is obtained integrating the momentum equation [second equation in Eqn. (13)], that after reordering reads as in Eqn. (30)

$$\frac{\partial}{\partial z} p = -\frac{\partial}{\partial t}(\rho_m v_m) - \frac{\partial}{\partial z}(\rho_m v_m v_m) - \frac{\partial}{\partial z}\left[\rho_m c_p \left(1-c_p\right) v_{pq}^2\right] + \rho_m \vec{g} \tag{30}$$

3.4 Determination of the front velocities

In addition to the semi-analytical solution obtained, two other valuable results can be obtained by the application of the Rankine-Hugoniot conditions (jump conditions) (LeVeque, 2002) in the system given by Eqn. (13). So that, applying the jump condition in each front (see Figure 2) we have Eqns. (31)-(32)

$$\begin{cases} \left(\rho_m^0 - \rho_g\right)\, a' = \rho_m^0 v_m - \rho_g v_m^+ \\ \left(-\rho_g v_m^+ + \rho_m v_m\right)\, a' = \rho_m^0 v_m^2 + [p]_a - \rho_m c_p \left(1-c_p\right) v_{pq}^2 - \rho_g \left(v_m^+\right)^2 \\ \left(\alpha_g^0 - 1\right)\, a' = \alpha_g \left[v_m + \left(1-c_p\right) v_{pq}^0\right] - v_m^+ \end{cases} \tag{31}$$

where a' is the velocity of the top front.

$$\begin{cases} \left(\rho_l - \rho_m^0\right)\, b' = -\rho_m^0 v_m \\ -\rho_m^0 v_m\, b' = -\rho_m^0 v_m^2 + [p]_b + \rho_m c_p \left(1-c_p\right) v_{pq}^2 \\ b' = v_m + \left(1-c_p\right) v_{pq}^0 \end{cases} \tag{32}$$

where b' is the velocity of the bottom front. Next, working with the first and third equations of (32) it is possible to isolate the velocity of the bottom front, which is shown in Eqn. (33)

$$b' = \left(1-\alpha_g^0\right)\, v_{pq}^0 \tag{33}$$

in the same way, working with the first and third equation of Eqn. (32) it is possible to isolate the value of a' which is given in Eqn. (34).

$$a' = -\alpha_g^0\, v_{pq}^0 \tag{34}$$

3.5 Solving examples

Now it is possible to apply the semi-analytical solution to a practical case. It consists in solving the Eqns. (28), (25) and (30) in the sequence shown in the Algorithm 1.

3.5.1 First example

The first example corresponds to which was proposed by Gastaldo *et al.* (Gastaldo et al., 2011) based on the work of Coquel *et al.* (Coquel et al., 1997). It consists in a sedimentation problem like that presented in Section 3. It has the particular characteristic of having a constant relative velocity, v_{pq}. This assumption is clearly non-physical but leads to a simple solution that qualitatively represents the original phenomenon.

The problem is set with $h = 7.5$, $\alpha_g = 0.5$, $v_m = 0$ and $p = 0$. The physical constants are $g = 9.81$, $\rho_l = 1000$ and $\rho_g = 1.2$, the viscosities are set to zero. The relative velocity has the value $v_{pq} = 1$. This selection for the relative velocity implies that in Eqn. (7) the constants have the values $v_{rc} = 1$ and $a = 0$. Finally the flux for the α_g results to be which as shown in Eqn. (35)

$$\mathrm{F}\left(\alpha_g\right) = v_{rc}\left(\alpha_g - \alpha_g^2\right) \tag{35}$$

being the flux derivative given by Eqn. (36)

$$\mathrm{F}'\left(\alpha_g\right) = v_{rc}\left(1 - 2\,\alpha_g\right) \tag{36}$$

allowing to determine the convexity or non-convexity of the flux and the eigenvalues. The graphs for both functions are shown in Figure 3. The shaded zone is the so-called *convex hull* which is used for wave analysis. From the graph it is possible to show that the flux function is convex. This leads to a solution having two shocks, one going from bottom to the top and the other one in the opposite direction. The convex hull is formed by two straight lines representing the two shocks. Using Eqns. (33)-(34) the front velocities are $a' = -0.5$ and $b' = 0.5$. The solutions for two different times are shown in Figure 4.

3.5.2 Second example

The second example introduces a decreasing linear law for the relative velocity, which allows a more rich physical behaviour. In this case the constants' values are: $v_{rc} = 1$ and $a = 1$. This is a simple law but gives physically meaningful results since the velocity decreases with α_g until zero, so that, the settling process ends once pure gas phase is reached. In addition $\rho_g = 1$ and $\rho_l = 1000$ are selected.

Under these assumptions the flux $\mathrm{F}\left(\alpha_g\right)$ results to be non-convex and compound waves can be formed. The laws for the flux and its derivative are given in Eqns. (37)-(38)

$$\mathrm{F}\left(\alpha_g\right) = v_{rc}\left(\alpha_g^3 - 2\,\alpha_g^2 + \alpha_g\right) \tag{37}$$

$$\mathrm{F}'\left(\alpha_g\right) = v_{rc}\left(3\,\alpha_g^2 - 4\,\alpha_g + 1\right) \tag{38}$$

Algorithm 1 Steps for semi-analytical solution

1. Solve the hyperbolic partial differential equation for α_g

$$\frac{\partial}{\partial t}(\alpha_g) + \frac{\partial}{\partial z}\left\{\alpha_g\left[\alpha_g\left(\frac{\rho_g}{\rho_m}-1\right)+\left(1-\frac{\alpha_g\,\rho_g}{\rho_m}\right)\right]v_{rc}\,(1-\alpha_g)^a\right\}=0$$

2. Find the mixture velocity using α_g and physical parameters

$$v_m = \alpha_g\left(\frac{\rho_g}{\rho_m}-1\right)v_{pq}$$

3. Finally, obtain the pressure integrating the momentum balance

$$\frac{\partial}{\partial z}p = -\frac{\partial}{\partial t}(\rho_m v_m) - \frac{\partial}{\partial z}(\rho_m v_m v_m) - \frac{\partial}{\partial z}\left[\rho_m c_p\,(1-c_p)\,{v_{pq}}^2\right] + \rho_m \vec{g}$$

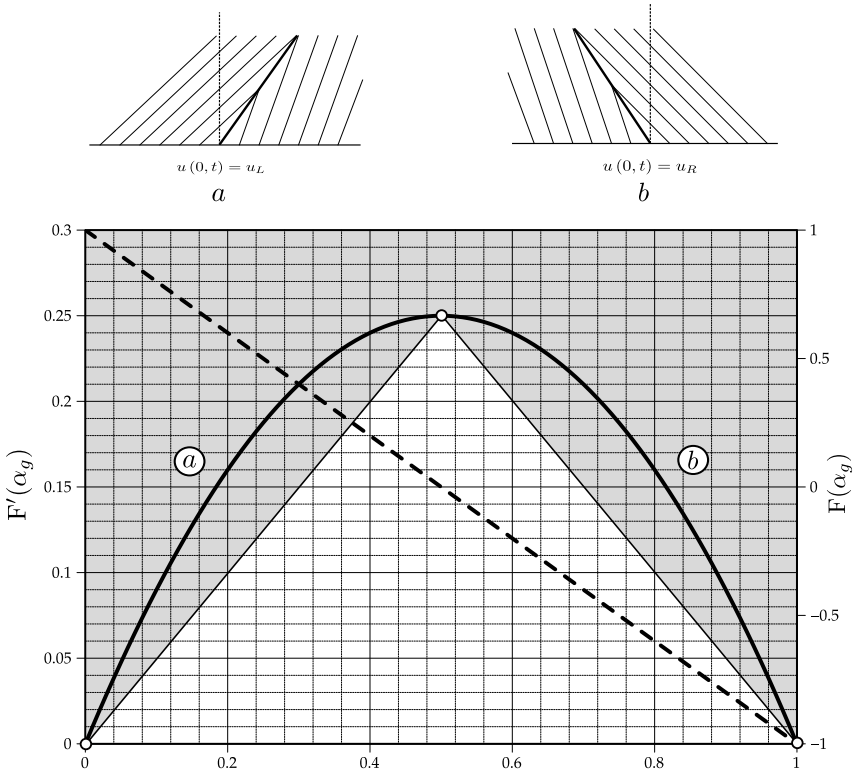

Figure 3: Riemann problem solutions for a convex flux. a. Right going shock, b. left going shock. ━━ flux, ▬ ▬ ▬ flux derivative

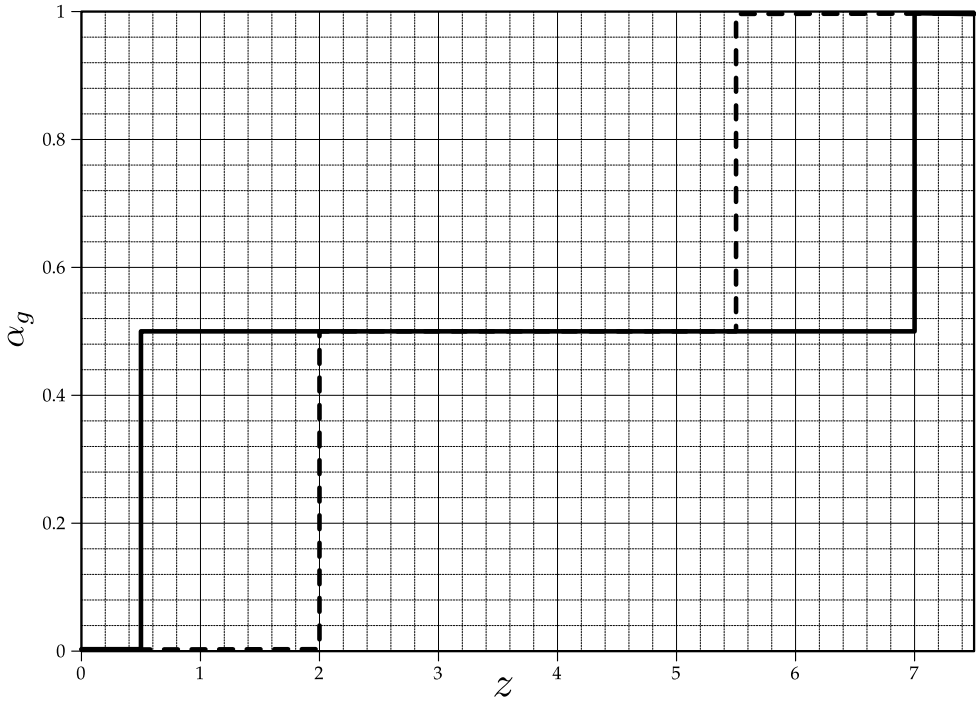

Figure 4: Riemann problem solutions for a convex flux with initial condition $\alpha_g = 0.5$ at time ——— 1 and – – – 4

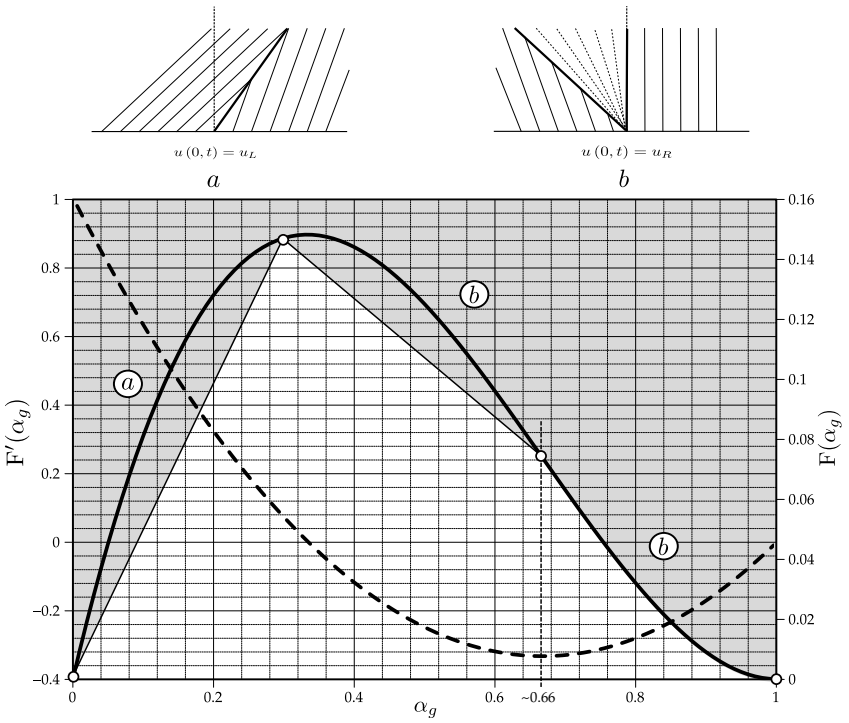

Figure 5: Riemann problem solutions for a non convex flux. a. Right going shock, b. left going rarefaction-shock. ——— flux, – – – flux derivative

In this case it is necessary to analyze the flux more deeply taking information from its first derivative. As is shown in Figure 5 the first derivative of the flux has a minimum so that the convexity changes from a concave flux to a convex flux. In order to detect the kind of waves present, the analysis inverts changing from the concave zone to the convex one, so in the change point compound waves can be present. In this case let's take the Riemann problem with initial conditions given by:

$$\mathrm{IC} : \alpha_g\left(z, 0\right) = 0.3$$

due to the convective velocity is ever positive α_g is transported from bottom to top giving place to two Riemann problems

$$\alpha_g\left(z, t\right) = \begin{cases} \alpha_{g_L} = 0, & z < b' t \\ \alpha_{g_R} = 0.3, & z > b' t \end{cases}$$

and

$$\alpha_g\left(z, t\right) = \begin{cases} \alpha_{g_L} = 0.3, & z < 1 - a' t \\ \alpha_{g_R} = \alpha_{g_{\mathrm{FAN}}}, & z > 1 - a' t \end{cases}$$

In Figure 5 the evolution goes through $\alpha_g = 0$, $\alpha_g = 0.3$ and $\alpha_g = 1$ crossing the inflection point $\alpha_g \cong 0.66$. The first change (a) from $\alpha_g = 0$ to $\alpha_g = 0.3$ evolves as a right going shock while the second change (b) has to be divided in two jumps, the first from $\alpha_g = 0.3$ to $\alpha_g \cong 0.66$ and the second from $\alpha_g \cong 0.66$ to $\alpha_g = 1$. The paths drawn by straight lines correspond to shocks and the paths that follow the flux curve are rarefactions. So that the second changes is a shock and then a rarefaction, or naming it in the direction of wave's velocity, a rarefaction-shock. The analytical solution of this problem is shown in Figure 6 for two different times. There, it is clearly seen the structure of the waves, note that the fan at the right side evolves from $\alpha_g \cong 0.66$ to $\alpha_g = 1$.

The second step is fulfilled applying the Eqn. (25) to the solution for α_g, which is shown in Figure 7. Finally, the pressure is obtained by the integration of the momentum equation giving the results shown in Figure 8. Respect to the velocity of the fronts, they are, $a' = -0.21$ and $b' = 0.49$. The first velocity is only indicative, due the wave is not a pure shock but a rarefaction-shock. These values can be verified in the figure.

4 AN EIGENVALUE-BASED SOLVER

Being addressed the main difficulties in solving the 1D ASMM system in Eqn. (13) and with a reference solution it is possible to devise an algorithm to solve it. It has to be able to manage the incompressibility and to use the restriction given by the continuity equation for the mixture in order to find the pressure p and the velocity v_m. In addition, the solution of the secondary phase mass conservation equation (the equation for α_g), which is nonlinear and hyperbolic requires the information of the eigenvalues and the solution of Riemman problems. Finally the boundedness of α_g has to be warranted in order not to obtain unphysical values for the mixture density ρ_m.

The start point in this task is the work of Brennan (Brennan, 2001) which is the base of the `settlingFoam` solver included in the OpenFOAM®(Weller et al., 1998) suite. The work

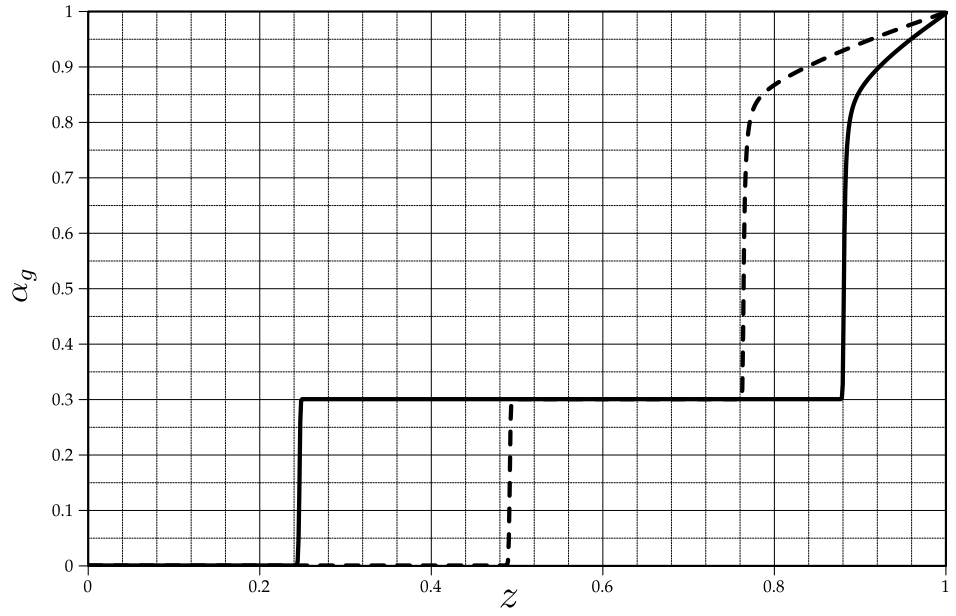

Figure 6: Riemann problem solutions for a non convex flux with initial condition $\alpha_g = 0.3$ at time ——— 0.5 and - - - 1

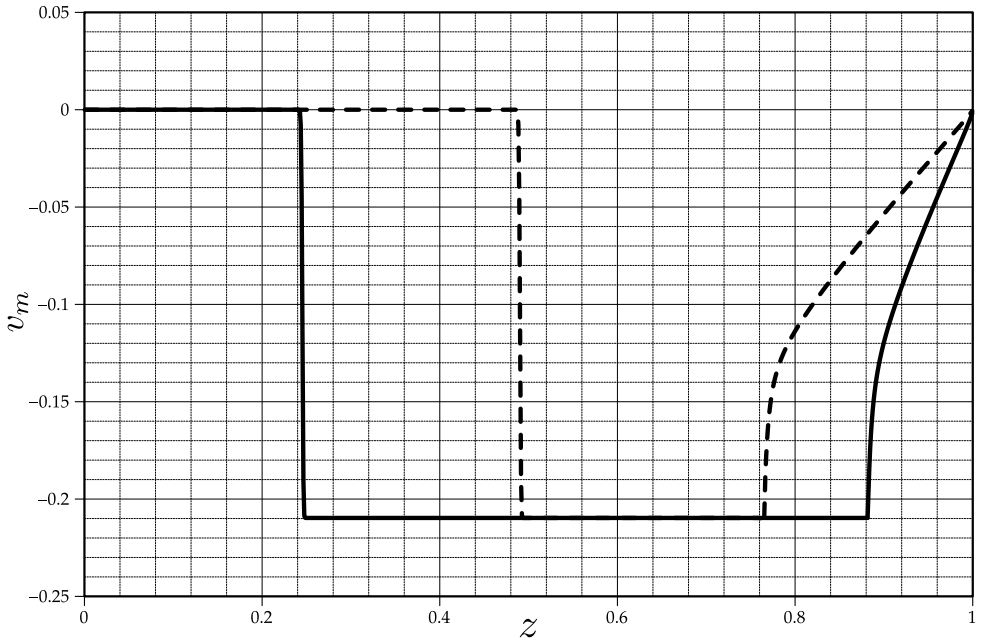

Figure 7: Mean velocity, v_m, profiles corresponding α_g distributions in previous figure at time ——— 0.5 and - - - 1

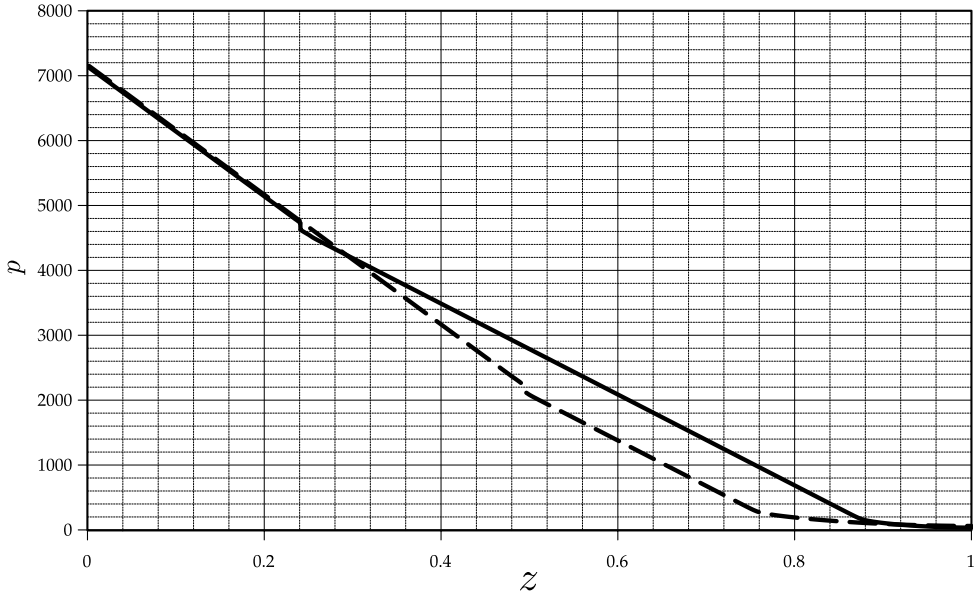

Figure 8: Pressure, p, profiles corresponding α_g and v_m distributions in previous figures at time ——— 0.5 and - - - 1

of Bohorquez (Bohorquez R. de M., 2008) gives additional clues in the topic. Both solvers rely on the PISO method (Issa, 1986) in order to solve the incompressibility using the Cell-centered Finite Volume Method (FVM) (Jasak, 1996). The treatment of the α_g equation is done as in Brennan's work taking into account the conservation of the mass flux, which ensures the boundedness in the solution of this equation. To do that, α_g equation is rewritten as is indicated in Eqns. (39)-(41)

$$\frac{\partial}{\partial t}(\alpha_g) + \frac{\partial}{\partial z}\left\{\alpha_g \left[v_m + (1 - c_p)\, v_{pq}\right]\right\} = 0 \tag{39}$$

$$\frac{\partial}{\partial t}\alpha_g\rho_g + \frac{\partial}{\partial z}\left\{\frac{\alpha_g\rho_g}{\rho_m}\left[\rho_m\, v_m + \rho_m\ (1 - c_p)\, v_{pq}\right]\right\} = 0 \tag{40}$$

$$\frac{\partial}{\partial t} A\,\rho_m + \frac{\partial}{\partial z}\left\{A\left[\rho_m\, v_m + \rho_m\ (1 - c_p)\, v_{pq}\right]\right\} = 0 \tag{41}$$

where $A = \frac{\alpha_g\rho_g}{\rho_m}$ and the term $\rho_m\, v_m$ is the indicated mass flux, this flux is obtained at each time-step by the PISO loop and is calculated at faces. In order to ensure boundedness and mass conservation this flux is used in A equation when it is discretized at faces by FVM. This equation retains the eigenvalues structure of the original α_g equation, which is crucial in the stabilization of the advective term. The solution is achieved by two *Riemann-free* solvers, namely the Downwind/Upwind method (L.F.Barceló et al., 2010; Márquez Damián, 2012) and a novel approach based on the Kurganov & Tadmor scheme (Kurganov and Tadmor, 2000; Márquez Damián, 2012) capable to use the given mass flux, $\rho_m v_m$, at faces.

Next is a description of the solver presented in Algorithm 2. The reader is referred to the cited works in order to be familiar with the notation of the FVM and basic algorithms for incompressible flows and hyperbolic equations. It starts with a prediction of mixture density based on the conservative mass flux $\Phi^0_{\rho_m \vec{v}_m}$ (step 1). This prediction is performed only in the two first

steps as is explained is step 4.

Next, in step 2 the relative velocity of dispersed phase respect to continuum phase $\vec{v}_{pq}{}^{0}$ is calculated using data from previous time-step. The momentum predictor needed for PISO loop is performed in step 3, where temporal, convective and viscous term are treated implicitly and gravitational, pressure and drift terms are treated explicitly using previous time-step data. This step gives $\tilde{\vec{v}}_m$.

In step 4 the volume fraction is advected through the use of the variable $A = \alpha_g \rho_g / \rho_m$, [Eqn.(41)] it allows to use the conservative mass flux which guarantees keeping α_g in a valid interval of [0, 1], next ρ_m is corrected by the first time. Since α_g is obtained from A which is not the conserved quantity in Eqn.(41), it requires a prediction of ρ_m at next time-step, in order to isolate A. Following the ideas of Gastaldo *et al.* (Gastaldo et al., 2011) a *time shifting* is used in ρ_m. So that a prediction and the previous time-step mixture density are used in the first two time-steps and the previous, $\rho_m{}^{0}$, and two steps before, $\rho_m{}^{-1}$, mixture densities are used in the rest of the run. This method ensures the mass conservation, which is crucial for the $v_m - p$ coupling.

The step 5 performs the PISO loop which has four sub-steps. First of all a new mass flux is calculated from the predicted $\tilde{\vec{v}}_m$ velocity, $\Phi^{\nu}{}_{\rho_m \vec{v}_m}$ which will be corrected along the PISO iterations. This flux is assembled following the spirit of Rhie-Chow interpolation (Rhie and Chow, 1983; Jasak, 1996; Peng Karrholm, 2008) and allows to have a velocity associated magnitude defined at faces while the pressure is defined at cell centres. This technique leads to a non oscillatory pressure solution (avoiding the pressure checkerboarding). Once the flux is calculated, a pressure equation is assembled from momentum equation and the mixture density conservation equation is solved for $p_i{}^{\nu}$, where ν is the number of PISO iteration. The second sub-step is to correct the mass flux, next in the third sub-step $\rho_m{}^{\nu}$ is corrected for the present iteration, while the $\vec{v}_m{}^{\nu}$ is corrected in the last sub-step.

So that at the end of the time-step ρ_m, $\vec{v}_m$, α_g and p have been updated and a new conservative mass flux $\Phi_{\rho_m \vec{v}_m}$ has been assembled.

4.1 Numerical results

The presented solver was applied to the cases explained in the previous section in order to check the solver functionality. So that, Algorithm 2 was implemented in `octave-of` an 1D emulator of OpenFOAM® written in octave (Márquez Damián et al., 2012). As regards to the first example, which is set as a simplified sedimentation case with two shocks, the results are compared with the solution given in the reference as is shown in Figure 9, these results were obtained with the Downwind/Upwind method. The main aspects of the comparison rely on the proper capturing of the shape of wave fronts and their velocity, in addition a correct steady state has to be reached. The numerical results present good agreement with the reference's results and with the theoretical solution (see Figure 4).

Respect to the second example it presents compound waves, again, the shape and velocity of the waves have to be predicted. The comparison between theoretical and numerical results is given in Figures 10-12. As is shown, the results have excellent agreement with the semi-analytical solution, particularly in the pressure. These results were obtained with the modified Kurganov & Tadmor scheme previously cited.

Algorithm 2 Segregated mixture solver with conserved flux

1. Solve ρ_m conservation equation for $\tilde{\rho}_m$ (ρ_m predictor, first two time-steps)

$$\frac{\tilde{\rho_m}_i - {\rho_m}^0{}_i}{\Delta t} V_i + \sum_f {\Phi^0}_{\rho_m \vec{v}_m} = 0$$

where ${\Phi^0}_{\rho_m \vec{v}_m} = {\rho_m}^0{}_f \, {\vec{v}_m}^0{}_f \cdot \vec{S}_f$ is the conserved mass flux, Δt the time-step, V_i the volume of the i-eth cell and $\vec{S}_f$ the face area vector.

2. Calculate relative velocities, ${\vec{v}_{pq}}^0$.

3. Solve momentum equation for $\tilde{\vec{v}}_m$ (momentum predictor)

$$\frac{\tilde{\rho_m}_i \tilde{\vec{v}}_{m\,i} - {\rho_m}^0{}_i {\vec{v}_m}^0{}_i}{\Delta t} V_i + \sum_f {\Phi^0}_{\rho_m \vec{v}_m} \tilde{\vec{v}}_{m\,f} \cdot \vec{S}_f = \left\{ -\vec{\nabla} p_{0i} + \tilde{\rho_m}_i \vec{g} - \vec{\nabla} \cdot \left[\tilde{\rho_m}_i {c_p}^0{}_i \left(1 - {c_p}^0{}_i\right) {\vec{v}_{pq}}^0 {\vec{v}_{pq}}^0 \right] \right\} V_i$$

where $\vec{\nabla}$ is the nabla discrete operator, so that $\vec{\nabla} a = \frac{1}{V} \sum_f a_f \cdot \vec{S}_f$ and $\vec{\nabla} \cdot \vec{b} = \frac{1}{V} \sum_f \vec{b}_f \cdot \vec{S}_f$

4. Solve for $A_g = \alpha_g \rho_g / \rho_m$ using the secondary phase conservation equation with conservative mass flux, ${\Phi^0}_{\rho_m \vec{v}_m}$. Then, obtain α_g and mixture density first correction, $\rho_m^{\check{}}$

$$\frac{{\rho_m}^a{}_i A_i - {\rho_m}^b{}_i {A^0}_i}{\Delta t} V_i + \sum_f {\Phi^0}_A \, A_f = 0$$

$$\rho_m^{\check{}}{}_i = \frac{\rho_l}{1 + \left(\frac{\rho_l}{\rho_g} - 1 \right) A_i} \qquad \alpha_{g\,i} = \frac{\rho_{m_i} A_i}{\rho_g}$$

where ${\Phi^0}_A = {\Phi^0}_{\rho_m \vec{v}_m} + \left(\tilde{\rho_m} \vec{v}_{\mathrm{dr},p} \right)_f \cdot \vec{S}_f$. ${\rho_m}^a = \tilde{\rho_m}$ and ${\rho_m}^b = {\rho_m}^0$ in two first time-steps and ${\rho_m}^a = {\rho_m}^0$ and ${\rho_m}^b = {\rho_m}^{-1}$ in the rest of the run

5. Do the PISO loop $0 < \nu <$ `nCorrectors` times. a) Solve pressure equation for p^ν $0 < \tau <$ `nNonOrthogonalCorrectors` times

$$\vec{\nabla} \cdot \left[\left(\frac{1}{\mathcal{A}_D} \right)_f \vec{\nabla} {p_i}^\nu \right] = \frac{{\rho_m}^\nu{}_i - {\rho_m}^0{}_i}{\Delta t} V_i + \sum_f {\Phi^\nu}_{\rho_m \vec{v}_m}$$

where if the momentum equation is discretized as $a_P v_{mP} + \sum_N a_N v_{mN} = c + d$, with c given by temporal, viscous and drift terms and d with gravitational and pressure terms, then $\mathcal{A}_D = \frac{a_P}{V_i}$ and $\mathcal{A}_H = \frac{-\sum_N a_N {v_m}^\nu{}_P + c}{V_i}$. In addition $\left[{\Phi^\nu}_{\rho_m \vec{v}_m} \right]_U = {\rho_m}^\nu{}_f \left({\vec{v}_m}^\nu{}_i \right)_f$, ${\Phi^\nu}_{\rho_m \vec{v}_m} = \left[{\Phi^\nu}_{\rho_m \vec{v}_m} \right]_U + {\rho_m}^\nu{}_f \left(\frac{1}{\mathcal{A}_D} \right)_f \vec{g} \cdot \vec{S}_f$ and ${\vec{v}_m}^\nu{}_i = \frac{\mathcal{A}_H}{\mathcal{A}_D}$. b) Correct the flux

$${\Phi^\nu}_{\rho_m \vec{v}_m} = {\Phi^\nu}_{\rho_m \vec{v}_m} - \sum_f \left(\frac{1}{\mathcal{A}_D} \right)_f \vec{\nabla} {p_i}^\nu$$

c) Do the ν correction for ${\rho_m}^\nu{}_i$ solving the mixture density conservation equation

$$\frac{{\rho_m}^\nu{}_i - {\rho_m}^0{}_i}{\Delta t} V_i + \sum_f {\Phi^\nu}_{\rho_m \vec{v}_m} = 0$$

d) Correct ${\vec{v}_m}^\nu{}_i$ at cell centres

$${\vec{v}_m}^\nu{}_i = {\vec{v}_m}^\nu{}_i + \frac{1}{\mathcal{A}_D} \mathcal{R} \left[\left({\Phi^\nu}_{\rho_m \vec{v}_m} - \left[{\Phi^\nu}_{\rho_m \vec{v}_m} \right]_U \right) \left(\frac{\mathcal{A}_D}{{\rho_m}^{\nu-1}} \right)_f \right]$$

where $\mathcal{R}(\Phi)$ is a face-to-cell field reconstruction operation.

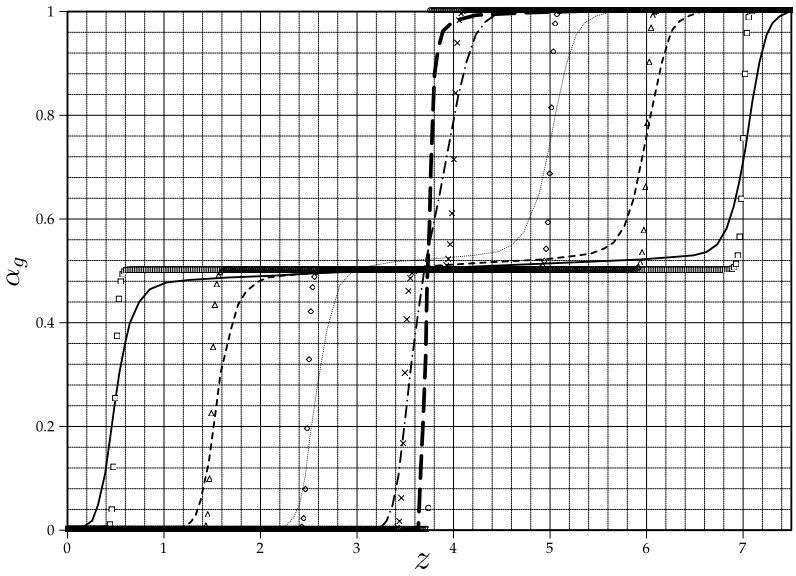

Figure 9: α_g profiles for two different times. Reference: ——— 1, - - - - - - 3, ... 5, —·—·— 7, ▬ ▬ ▬ 10. Present solver: □ 1, △ 3, ◊ 5, × 7, ○ 10

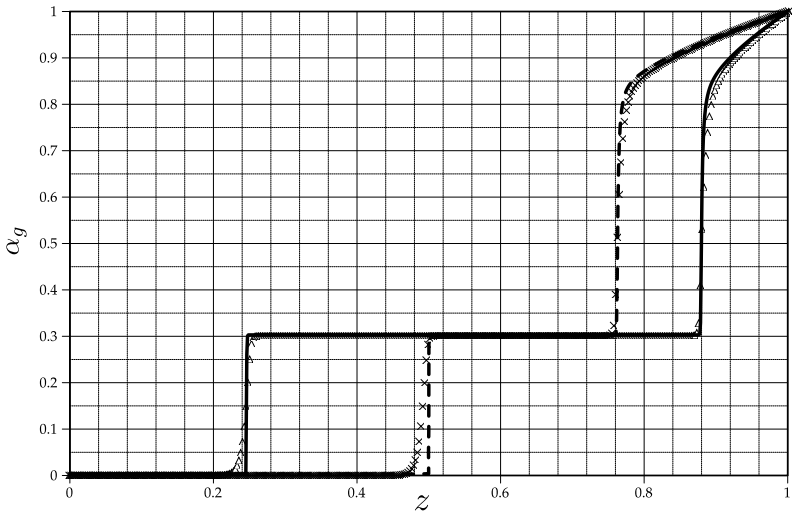

Figure 10: α_g profiles for two different times. ▬▬ 0.5 exact, ▬ ▬ ▬ 1 exact, △ 0.5 present solver, × 1 present solver

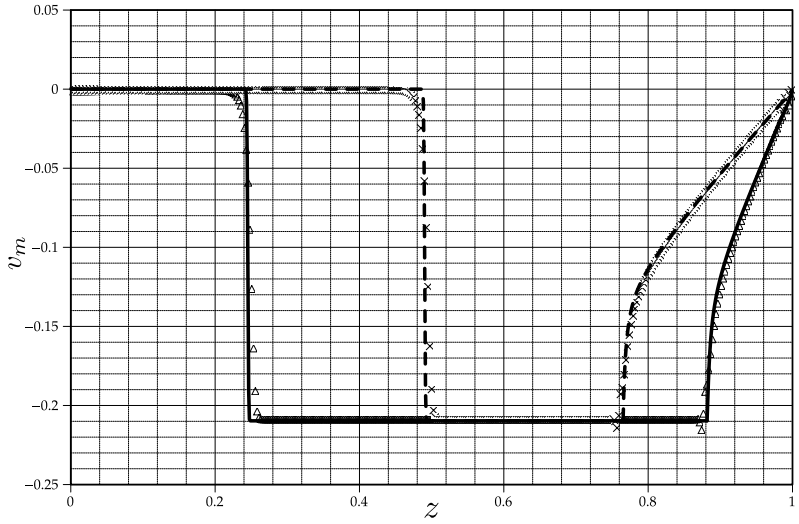

Figure 11: v_m profiles for two different times. ——— 0.5 exact, – – – 1 exact, $\triangle$ 0.5 present solver, $\times$ 1 present solver

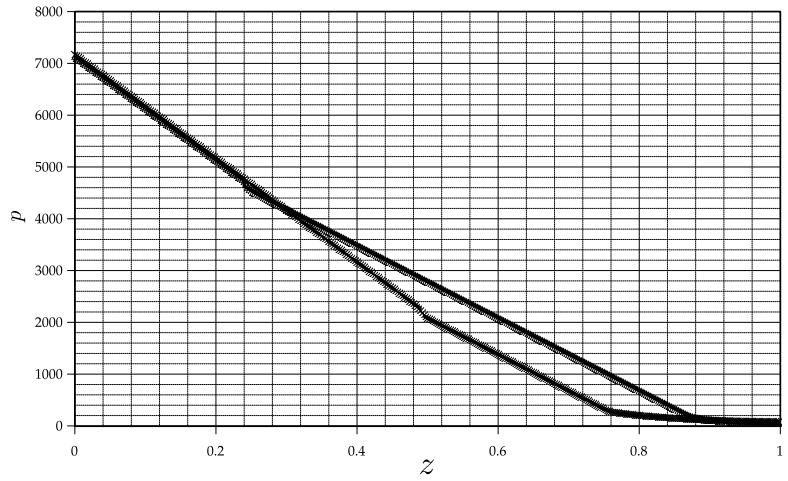

Figure 12: p profiles for two different times. ——— 0.5 exact, – – – 1 exact, $\triangle$ 0.5 present solver, $\times$ 1 present solver

5 CONCLUSIONS

After a review of the ASMM and taking the appropriate hypothesis a semi-analytical one dimensional solution for a sedimentation problem was developed. As in the original model, the selection of the flux function for the secondary phase has a principal role in the solution. This function is related with the relative velocity between phases representing the principal parameter of the settling process. The development of this solution is a contribution to the validation of ASMM solvers and to the modelization of two-phase flows. An in-deep analysis of the cases represented by additional flux functions in the secondary phase transport equation is a part of the future work.

The most important issues in solving this kind of systems were addressed and managed, they are: the incompressibility, the necessity of a bounded solution for the secondary phase transport equation and the hyperbolic nature of this equation, which leads to solutions with different kind of waves. To this end a PISO like method was implemented and tested. The integration of the secondary phase transport equation was done by means of previously developed methods available in the references.

Finally, the solver was tested against the proposed semi-analytical solution and a solution from the literature and good agreement was found, showing its reliability. In addition these results show that a group of sedimentation problems can modeled by the ASMM giving similar solutions respect to the Two-Fluid model.

As was stated the future work includes the formalization of the ASMM using the proposed kind of flux functions giving a relationship with other physical phenomena. In addition the extension of the present solver to two and three dimensions is also an objective.

5.1 Acknowledgement

The authors wish to give thanks to CONICET, Universidad Nacional del Litoral and ANPCyT for their financial support through grants PICT 1645 BID (2008) and CAI+D 65-333 (2009) and other financial resources. The collaboration between CIMEC and ICMC has been possible thanks to the CONICET/FAPESP International Cooperation Agreement.

An special acknowledgment is given to OpenFOAM®, gdb, octave and Paraview® developers and users community for their contribution to free software.

REFERENCES

Babik F., Gallouët T., Latché J., Suard S., and Vola D. On two fractional step finite volume and finite element schemes for reactive low mach number flows. In *The International Symposium on Finite Volumes for Complex Applications IV-Problems and Perspectives-Marrakech*. 2005.

Bohorquez R. de M. P. *Study and Numerical Simulation of Sediment Transport in Free-Surface Flow*. Ph.D. thesis, Málaga University, Málaga, 2008.

Brennan D. *The Numerical Simulation of Two-Phase Flows in Settling Tanks*. Ph.D. thesis, Department of Mechanical Engineering Imperial College of Science, Technology and Medicine, 2001.

Buscaglia G., Bombardelli F., and Garcia M. Numerical modeling of large-scale bubble plumes accounting for mass transfer effects. *International journal of multiphase flow*, 28(11):1763–1785, 2002.

Coquel F., El Amine K., Godlewski E., Perthame B., and Rascle P. A numerical method using upwind schemes for the resolution of two-phase flows. *Journal of Computational Physics*, 136(2):272–288, 1997.

Gastaldo L., Herbin R., and Latché J. An entropy preserving finite-element/finite-volume pressure correction scheme for the drift-flux model. *Arxiv preprint arXiv:0803.2469*, 2008.

Gastaldo L., Herbin R., and Latché J. A discretization of the phase mass balance in fractional step algorithms for the drift-flux model. *IMA Journal of Numerical Analysis*, 31(1):116–146, 2011.

Ishii M. Thermo-Fluid Dynamic Theory of Two-phase Flow. *NASA STI/Recon Technical Report A*, 75, 1975.

Ishii M. and Hibiki T. *Thermo-fluid dynamics of two-phase flow*. Springer Verlag, 2010.

Issa R. Solution of Implicitly Discretised Fluid Flow Equations by Operator Splitting. *J. Comput. Phys.*, 62:40–65, 1986.

Jasak H. *Error analysis and estimation for the finite volume method with applications to fluid flows*. Ph.D. thesis, Department of Mechanical Engineering Imperial College of Science, Technology and Medicine, 1996.

Knio O., Najm H., and Wyckoff P. A semi-implicit numerical scheme for reacting flow: Ii. stiff, operator-split formulation. *Journal of Computational Physics*, 154(2):428–467, 1999.

Kurganov A. and Tadmor E. New high-resolution central schemes for nonlinear conservation laws and convection–diffusion equations. *Journal of Computational Physics*, 160(1):241–282, 2000.

LeVeque R. *Finite volume methods for hyperbolic problems*. Cambridge Univ Pr, 2002.

L.F.Barceló, P.A. C., Larreteguy A., Gayoso R., Gayoso F., and Lavalle G. Análisis del comportamiento de equipos separadores de agua-petróleo usando volúmenes finitos y el modelo de drift-flux. In *Mecánica Computacional Vol XXIX (2010)*, pages 8463–8480. 2010.

Manninen M., Taivassalo V., and Kallio S. *On the mixture model for multiphase flow*. Technical Research Centre of Finland, 1996.

Márquez Damián S. *An Extended Mixture Model for the Simultaneous Treatment of Short and Long Scale Interfaces*. Ph.D. thesis, Facultad de Ingeniería y Ciencias Hídricas, Universidad Nacional del Litoral, 2012.

Márquez Damián S., Corzo S., and Nigro N. octave-of Octave 1D emulator of OpenFOAM(R). http://http://code.google.com/p/octave-of/, 2012.

Najm H., Wyckoff P., and Knio O. A semi-implicit numerical scheme for reacting flow: I. stiff chemistry. *Journal of Computational Physics*, 143(2):381–402, 1998.

Peng Karrholm F. *Numerical Modelling of Diesel Spray Injection, Turbulence Interaction and Combustion*. Ph.D. thesis, Chalmers University of Technology, Goteborg, 2008.

Qian F., Huang Z., Chen G., and Zhang M. Numerical study of the separation characteristics in a cyclone of different inlet particle concentrations. *Computers & chemical engineering*, 31(9):1111–1122, 2007.

Rhie C.M. and Chow W.L. Numerical study of the turbulent flow past an airfoil with trailing edge separation. *AIAA Journal*, 21(11):1525–1532, 1983.

Schiller L. and Naumann Z. A drag coefficient correlation. *Z. Ver. Deutsch. Ing.*, 77:318, 1935.

Toro E. *Riemann solvers and numerical methods for fluid dynamics: a practical introduction*. Springer Verlag, 2009.

Weller H., Tabor G., Jasak H., and Fureby C. A Tensorial Approach to Computational Continuum Mechanics Using Object-oriented Techniques. *Computers in physics*, 12:620, 1998.

Zeidan D. The riemann problem for a hyperbolic model of two-phase flow in conservative form. *International Journal of Computational Fluid Dynamics*, 25(6):299–318, 2011.

Zeidan D. and Slaouti A. Validation of hyperbolic model for two-phase flow in conservative form. *International journal of computational fluid dynamics*, 23(9):623–641, 2009.